*Ultrasound Obstet Gynecol* 2012; **39**: 726–728
Published online 9 May 2012 in Wiley Online Library (wileyonlinelibrary.com).

# Letters to the Editor

## Prenatal genetic confirmation of a *COL4A1* mutation presenting with sonographic fetal intracranial hemorrhage

While the antenatal onset of intracranial lesions associated with *COL4A1* has been reported by us and others, this diagnosis has always been made after birth[1–3] (Table S1). This is the first report of the diagnosis of a mutation in the *COL4A1* gene in a fetus. A 35-year-old woman was referred after detection of a cystic lesion in the fetal posterior cranial fossa during ultrasound screening. She had no family history of anomalies or recent history of maternal or fetal trauma. Screening for TORCH and alloimmune antithrombocyte antibodies in maternal plasma, and polymerase chain reaction (PCR) for cytomegalovirus and quantitative fluorescent (QF)-PCR for trisomies 13, 18 and 21 in amniotic fluid were negative. Fetal neurosonography at 21 + 6 weeks' gestation revealed hyperechogenic walls of the lateral ventricles and left-sided periventricular echogenicity. A large germinal matrix hemorrhage extended with a wedge-shaped echogenic lesion into the left thalamus. The left cerebellar hemisphere was replaced by an echolucent area with displacement of the right cerebellar hemisphere (Figure 1a). At 23 + 4 weeks, fetal MRI confirmed the ultrasound findings. The posterior fossa mass had expanded and had the appearance of an organizing hematoma with destruction of the left cerebellar hemisphere (Figures 1b and c). Repeat ultrasound scans showed mild progressive dilatation, more obvious echogenicity of the lateral ventricles and wedge-shaped cystic evolution of the left thalamus (Figure S1a).

By 30 weeks' gestation the results of sequence analysis of the *COL4A1* gene using fetal DNA isolated from amniotic fluid became known, showing a *de-novo* pathogenic missense mutation (G1103R). At 41 + 6 weeks a female infant was delivered vaginally with normal Apgar scores, birth weight (3355 g) and head circumference (34 cm). Neonatal MRI confirmed a wedge-shaped area of cavitation in the left basal ganglia. There was lack of myelination of the posterior limb of the internal capsule and absence of the left cerebellar hemisphere (Figures S1b and c). Ophthalmological investigation showed sporadic small retinal hemorrhages. Renal sonography was normal. The infant developed a hemiplegia.

Rates of fetal intracranial hemorrhage of 0.46 per 1000 deliveries and 0.9 per 1000 pregnancies have been reported at referral centers[4]. In an unknown proportion of fetuses, a Mendelian genetic disorder, associated with an increased risk for cerebral arteriopathy, can be detected. The *COL4A1* gene encodes for the alpha-1 chain of type IV collagen, a basement membrane protein, which is expressed widely in all tissues, including the vasculature[5]. Mutations in the *COL4A1* gene lead to an altered COL4A1 protein, which compromises the basement membrane of the vasculature, thus predisposing to hemorrhage. In 2005 Gould *et al.*[6] were the first to report *COL4A1* mutations in mice with perinatal hemorrhage and in human families with porencephaly. Since then *COL4A1* mutations have been reported in association with a wide spectrum of symptoms, including familial porencephaly, intracranial aneurysms, muscle cramps, hemorrhagic stroke, infantile hemiparesis[7–9] and intraventricular hemorrhage in preterm infants with parenchymal hemorrhage of antenatal onset[2,3,10]. More extensive supratentorial lesions, in combination with cerebellar injury, have recently been reported[2]. In our case, the combination of a supratentorial hemorrhage and a cerebellar lesion led to prenatal diagnosis of a

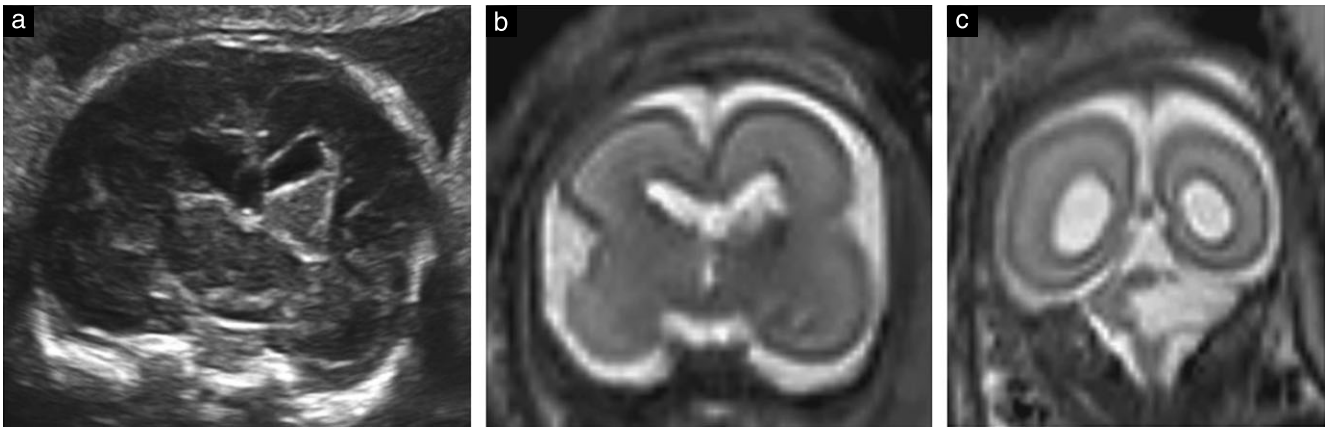


**Figure 1** (a) Prenatal coronal ultrasound image at 21 + 6 weeks' gestation showing a wedge-shaped echogenic lesion of the thalamus adjacent to the left lateral ventricle. (b) Prenatal coronal T2SE-weighted magnetic resonance image (MRI) at 23 + 4 weeks' gestation, confirming the lesion and showing a low-signal-intensity area at the border, suggestive of a hemorrhagic component. (c) Prenatal MRI at 23 + 4 weeks' gestation, showing the absent left cerebellar hemisphere on posterior coronal view.

*COL4A1* mutation. Making this diagnosis has important implications for perinatal management and genetic counseling.

K. D. Lichtenbelt†, L. R. Pistorius*‡, S. M. De Tollenaer§, G. M. Mancini¶ and L. S. De Vries**
†*Department of Medical Genetics, Division of Biomedical Genetics, University Medical Center Utrecht, Utrecht, The Netherlands;* ‡*Department of Obstetrics and Gynecology, University Medical Center Utrecht, Utrecht, The Netherlands;* §*Department of Neonatology, Isala Clinics, Zwolle, The Netherlands;* ¶*Department of Clinical Genetics, Erasmus University MC/Sophia Children's Hospital, Rotterdam, The Netherlands;* ***Department of Neonatology, University Medical Center Utrecht, Utrecht, The Netherlands*
**Correspondence.*
*Wilhelmina Children's Hospital KE 04.123.1, University Medical Center Utrecht, PO Box 85 090, 3508 AB, Utrecht, The Netherlands*
*(e-mail: L.Pistorius@umcutrecht.nl)*
**DOI:** 10.1002/uog.11070

## References

1. de Vries LS, Koopman C, Groenendaal F, Van Schooneveld M, Verheijen FW, Verbeek E, Witkamp TD, van der Worp HB, Mancini G. COL4A1 mutation in two preterm siblings with antenatal onset of parenchymal hemorrhage. *Ann Neurol* 2009; **65**: 12–18.
2. Meuwissen ME, de Vries LS, Verbeek HA, Lequin MH, Govaert PP, Schot R, Cowan FM, Hennekam R, Rizzu P, Verheijen FW, Wessels MW, Mancini GM. Sporadic COL4A1 mutations with extensive prenatal porencephaly resembling hydranencephaly. *Neurology* 2011; **76**: 844–846.
3. Vermeulen RJ, Peeters-Scholte C, Van Vught JJ, Barkhof F, Rizzu P, van der Schoor SR, van der Knaap MS. Fetal origin of brain damage in 2 infants with a COL4A1 mutation: fetal and neonatal MRI. *Neuropediatrics* 2011; **42**: 1–3.
4. Elchalal U, Yagel S, Gomori JM, Porat S, Beni-Adani L, Yanai N, Nadjari M. Fetal intracranial hemorrhage (fetal stroke): does grade matter? *Ultrasound Obstet Gynecol* 2005; **26**: 233–243.
5. Pöschl E, Schlötzer-Schrehardt U, Brachvogel B, Saito K, Ninomiya Y, Mayer U. Collagen IV is essential for basement membrane stability but dispensable for initiation of its assembly during early development. *Development* 2004; **131**: 1619–1628.
6. Gould DB, Phalan FC, Breedveld GJ, van Mil SE, Smith RS, Schimenti JC, Aguglia U, van der Knaap MS, Heutink P, John SW. Mutations in Col4a1 cause perinatal cerebral hemorrhage and porencephaly. *Science* 2005; **308**: 1167–1171.
7. Breedveld G, de Coo IF, Lequin MH, Arts WF, Heutink P, Gould DB, John SW, Oostra B, Mancini GM. Novel mutations in three families confirm a major role of COL4A1 in hereditary porencephaly. *J Med Genet* 2006; **43**: 490–495.
8. Vahedi K, Boukobza M, Massin P, Gould DB, Tournier-Lasserve E, Bousser MG. Clinical and brain MRI follow-up study of a family with COL4A1 mutation. *Neurology* 2007; **69**: 1564–1568.
9. Alamowitch S, Plaisier E, Favrole P, Prost C, Chen Z, Van Agtmael T, Marro B, Ronco P. Cerebrovascular disease related to COL4A1 mutations in HANAC syndrome. *Neurology* 2009; **73**: 1873–1882.
10. Bilguvar K, DiLuna ML, Bizzarro MJ, Bayri Y, Schneider KC, Lifton RP, Gunel M, Ment LR; Pacifier and Breastfeeding Trial Group. COL4A1 mutation in preterm intraventricular hemorrhage. *J Pediatr* 2009; **155**: 743–745.

### SUPPORTING INFORMATION ON THE INTERNET

The following supporting information may be found in the online version of this article:

**Table S1** Summary of prenatal ultrasound and magnetic resonance imaging findings in cases with a *COL4A1* mutation.

**Figure S1** (a) Prenatal ultrasound image at 32 + 4 weeks' gestation showing cystic evolution of the echogenic lesion into a porencephalic cyst. (b) Postnatal magnetic resonance imaging (T2SE-weighted), axial views. The left cerebellar hemisphere is absent. There is an area of cavitation in the left basal ganglia. (c) Myelination is only seen as low signal intensity in the right posterior limb of the internal capsule.

## Postpartum uterine involution: sonographic changes in the endometrium between 2 and 6 weeks postpartum related to delivery mode and gestational age at delivery

Ultrasound is the most appropriate tool with which to evaluate the postpartum uterus. Parameters such as the uterine anteroposterior (AP) diameter have been used as indicators of the state of involution[1,2]. Several studies on the relationship between sonographic morphological findings of the postpartum uterus and complications have been published[3–6]. However, few studies correlate changes in endometrial thickness with the state of involution. To the best of our knowledge, no study has examined whether postpartum changes in the endometrium depend on delivery mode or gestational age at delivery. We performed a study to define normal changes in endometrial thickness using sonography in the puerperium and to determine whether there is a difference in the changes depending on delivery mode and gestational age at delivery.

Ninety-five women who underwent vaginal or Cesarean deliveries of singletons at ≥ 32 weeks' gestation with normal puerperium participated in this prospective observational study. None had a morphological uterine abnormality or a postpartum hemorrhagic event. All women were asked to return to the hospital 2 and 6 weeks postpartum, when transabdominal sonography and transvaginal sonography were carried out, respectively. All ultrasound

**Table 1** Changes in uterine anteroposterior diameter and endometrial thickness, as determined sonographically between week 2 and week 6 postpartum in relation to delivery mode and time of delivery

| *Sonographic characteristic* | n* | *Delivery specifics* | | *Postpartum measurement (cm, mean ± SD)* | | | |
|---|---|---|---|---|---|---|---|
| | | *Mode* | *Time* | *Week 2* | *Week 6* | *Δ(cm)‡* | P† |
| Anteroposterior diameter | 39 | Vaginal | Term | 6.29 ± 0.94 | 3.23 ± 0.91 | 3.05 ± 1.19 | <0.0001 |
| | 10 | | Preterm | 5.08 ± 1.34 | 3.34 ± 0.70 | 1.74 ± 1.08 | 0.001 |
| | 26 | Cesarean | Term | 5.96 ± 0.82 | 3.48 ± 1.14 | 2.48 ± 1.11 | <0.0001 |
| | 20 | | Preterm | 5.59 ± 0.72 | 3.89 ± 1.20 | 1.71 ± 1.38 | 0.001 |
| Endometrial thickness | 39 | Vaginal | Term | 1.60 ± 0.79 | 0.73 ± 0.50 | 0.87 ± 0.71 | <0.0001 |
| | 10 | | Preterm | 1.58 ± 0.41 | 0.68 ± 0.44 | 0.92 ± 0.59 | 0.001 |
| | 26 | Cesarean | Term | 1.27 ± 0.64 | 0.79 ± 0.37 | 0.48 ± 0.54 | 0.002 |
| | 20 | | Preterm | 1.41 ± 0.72 | 0.78 ± 0.30 | 0.63 ± 0.64 | 0.001 |

*Number of women. †Student's *t*-test. ‡Difference between measurements made at week 2 and week 6.

examinations were performed using a commercially available real-time ultrasound machine (ACCUVIX QX, Medison, Korea) with a 4–7-MHz transabdominal convex probe and a 6.5-MHz transvaginal probe. Uterine measurements were obtained in a longitudinal section of the uterus. The maximum AP diameter and the maximum endometrial thickness were measured at 2 and 6 weeks postpartum. Both measurements were taken perpendicular to the endometrium.

Study volunteers were divided into four subgroups according to delivery mode and gestational age at delivery: term vaginal delivery, preterm vaginal delivery, term Cesarean delivery and preterm Cesarean delivery. We found that the decrease in AP diameter was smaller after a preterm delivery than that after a term delivery ($P = 0.003$ for vaginal delivery and $P = 0.056$ for Cesarean delivery), although the difference was not statistically significant for Cesarean deliveries. After a term delivery, the decrease in AP diameter was smaller after a Cesarean delivery than that after a vaginal delivery ($P = 0.054$), although this was not statistically significant. The decrease in endometrial thickness was similar, irrespective of delivery mode and gestational age at delivery (term vs. preterm) with one exception: the decrease was larger after a vaginal term delivery than after a Cesarean term delivery ($P = 0.040$) (Table 1). The AP diameter and endometrial thickness were both found to decrease between 2 and 6 weeks postpartum, but showed some differences in relation to delivery mode and gestational age at delivery.

From these results, we suggest that each parameter potentially contributes to an understanding of the process of involution in relation to delivery mode and gestational age at delivery.

H. S. Bae, K. H. Ahn, M. J. Oh, H. J. Kim and S. C. Hong*
*Department of Obstetrics and Gynecology, College of Medicine, Korea University, Seoul, Korea*
**Correspondence.*
*(e-mail: novak082@naver.com)*
**DOI:** 10.1002/uog.11069

## References

1. Wachsberg HR, Kurtz AB. Gas within the endometrial cavity at postpartum US: a normal finding after spontaneous vaginal delivery. *Radiology* 1992; **183**: 431–433.
2. Lavery JP, Shaw LA. Sonography of the puerperal uterus. *J Ultrasound Med* 1989; **8**: 481–486.
3. Hertzberg BS, Bowie JD. Ultrasound of the postpartum uterus. Prediction of retained placental tissue. *J Ultrasound Med* 1991; **10**: 451–456.
4. Mulic-Lutvica A, Axelsson O. Ultrasound finding of an echogenic mass in women with secondary postpartum hemorrhage is associated with retained placental tissue. *Ultrasound Obstet Gynecol* 2006; **28**: 312–319.
5. Zuckerman J, Levine D, McNicholas MM, Konopka S, Goldstein A, Edelman RR, McArdle CR. Imaging of pelvic postpartum complications. *AJR Am J Roentgenol* 1997; **168**: 663–668.
6. Pather S, Ford M, Reid R, Sykes P. Postpartum curettage: an audit of 200 cases. *Aust N Z J Obstet Gynaecol* 2005; **45**: 368–371.

 